

1 **Abundance of Oligoflexales bacteria is associated with algal**
2 **symbiont density independent of thermal stress in Aiptasia**
3 **anemones**

4 Emily G. Aguirre^{1*}, Marissa J. Fine¹, Carly D. Kenkel¹

5 ¹ Department of Biological Sciences, University of Southern California, 3616 Trousdale
6 Parkway, Los Angeles, CA 90089, United States of America

7 *Corresponding author:

8 Emily G Aguirre

9 Department of Biology

10 University of Southern California

11 3616 Trousdale Parkway

12 Los Angeles, CA 90026, USA

13 E-mail: emilyagu@usc.edu; emilygaguirre@gmail.com

14
15 Keywords: *Exaiptasia pallida*, *Symbiodinium*, anemone, symbiotic-state microbiome, thermal
16 stress, Oligoflexales, symbiont-host ratio

17

18

19

20

21

22

23

24

25

26

27

28

29

30

31 **ABSTRACT**

32 Many multicellular organisms, such as humans, plants, and invertebrates, depend on symbioses
33 with microbes for metabolic cooperation and exchange. Reef-building corals, an ecologically
34 important order of invertebrates, are particularly vulnerable to environmental stress in part
35 because of their nutritive symbiosis with dinoflagellate algae, and yet also benefit from these and
36 other microbial associations. While coral microbiomes remain difficult to study because of their
37 complexity, the anemone *Aiptasia* is emerging as a simplified model. Research has demonstrated
38 co-occurrences between microbiome composition and the abundance and type of algal symbionts
39 in cnidarians. However, whether these patterns are the result of general stress-induced shifts or
40 depletions of algal-associated bacteria remains unclear. Our study aimed to distinguish the effect
41 of changes in symbiont density and thermal stress on the microbiome of symbiotic *Aiptasia*
42 strain CC7 by comparing them with aposymbiotic anemones, depleted of their native symbiont,
43 *Symbiodinium linucheae*. Our analysis indicated that overall, thermal stress had the greatest
44 impact on disrupting the microbiome. We found that three bacterial classes made up most of the
45 relative abundance (60-85 %) in all samples, but the rare microbiome fluctuated between
46 symbiotic states and following thermal stress. We also observed that *S. linucheae* density
47 correlated with abundance of Oligoflexales, suggesting these bacteria may be primary symbionts
48 of the dinoflagellate algae. The findings of this study help expand knowledge on prospective
49 multipartite symbioses in the cnidarian holobiont and how they respond to environmental
50 disturbance.

51

52

53

54

55

56

57 INTRODUCTION

58 Biological organisms, from single cells to ecosystems, are influenced by symbiotic interactions
59 (Boucher, 1985; University of Massachusetts Amherst Massachusetts Lynn Margulis, Margulis
60 and Fester, 1991; Smith and Szathmary, 1997; Sachs *et al.*, 2004). Although symbioses are
61 generally modeled and studied as two-way interactions, multipartite symbioses are also
62 ubiquitous and have been well-documented in plants (Miransari, 2011; Antunes and Goss, 2015;
63 Adeniji, Babalola and Loots, 2020; Afkhami *et al.*, 2020), humans (Wahida, Tang and Barr,
64 2021), and invertebrates (Worthen, Gode and Graf, 2006; Ffrench-Constant, Eleftherianos and
65 Reynolds, 2007; Chaston and Goodrich-Blair, 2010; Stock, 2019). These multi-partner
66 interactions can provide the host with essential metabolites, amino acids, and vitamins
67 (Cleveland, Alan Verde and Lee, 2011; Adeniji, Babalola and Loots, 2020). Additionally, they
68 can also confer defense (Zan *et al.*, 2019), facilitate host morphogenesis (Wichard, 2015) and aid
69 resilience under environmental stress (Gupta *et al.*, 2021; Santoyo *et al.*, 2022).

70 Understanding the impact of multi-partner associations on the health and survival of
71 marine invertebrates is crucial given they are among the most susceptible animals to the impacts
72 of climate change (Mather, 2013; Lam *et al.*, 2020). The global decline of corals, which are
73 cnidarian hosts that harbor intracellular populations of dinoflagellate algae in the family
74 Symbiodiniaceae and other microbial associates (Pandolfi *et al.*, 2003) is already underway and
75 is predicted to worsen with climate change (Hoegh-Guldberg *et al.*, 2007; Allemand and Osborn,
76 2019; Kleypas and Kleypas, 2019). Bleaching, which involves the expulsion of symbiotic algae
77 in cnidarians resulting in the loss of color, can be induced by several factors, although elevated
78 temperature, as noted by (Douglas, 2003)), is the most common cause. Yet there is also abundant
79 variation in coral thermal tolerance evidenced by differences in bleaching among species,
80 populations, and individuals (Dixon *et al.*, 2015; Thomas *et al.*, 2018; Drury, 2020).
81 Collectively, these observations have led to the "Coral Probiotic Hypothesis" (Reshef *et al.*,
82 2006) which is based on the notion that symbiotic relationships with bacteria can increase coral
83 resilience (Peixoto *et al.*, 2017).

84 The cnidarian-dinoflagellate symbiosis is better characterized in the literature than
85 potential cnidarian-bacterial symbioses, and it remains unclear whether environmental or internal

86 host factors, like host genetics or microalgal symbiont type, modulate the composition of
87 cnidarian microbiomes (Bourne, Morrow and Webster, 2016; van Oppen and Blackall, 2019;
88 Barno *et al.*, 2021). One understudied theory postulates that well-known cnidarian-bacterial
89 associates may actually be primary associates of Symbiodiniaceae, in both free-living and in-
90 hospite states (Ritchie, 2012; Bernasconi *et al.*, 2019; Matthews *et al.*, 2020). Global datasets
91 suggest that the identity of Symbiodiniaceae may contribute to structuring coral and anemone
92 microbiomes (Bernasconi *et al.*, 2019). For instance, susceptibility to *Vibrio* pathogens was
93 higher in *Acropora cytherea* corals hosting *Symbiodinium* than *Durusdinium* (formerly Clade A
94 and D *Symbiodinium*, respectively) (Rouzé *et al.*, 2016). Additionally, the abundance of
95 diazotrophs in *Montipora* corals also correlated with algal symbiont type (Olson *et al.*, 2009).
96 Similarly, unique microbiomes were identified in symbiotic and aposymbiotic *Aiptasia*
97 anemones (Herrera *et al.*, 2017) indicating presence of the symbiont influences the microbiome.
98 However, insufficient evidence exists to verify this hypothesis and tracking bacteria in adult
99 corals is nearly impossible, due to their high bacterial diversity (Blackall, Wilson and van
100 Oppen, 2015), which poses a challenge for distinguishing obligatory and facultative bacterial
101 symbionts. Furthermore, selectively eliminating holobiont members empirically is not feasible
102 since reef-building corals cannot survive without their algal symbionts, who provide vital sugars
103 and nutrients (Weis, 2008). The anemone *Aiptasia* (*Exaiptasia pallida*, *sensu stricto*) is a
104 tractable model for studying the cnidarian microbiome as it harbors fewer bacterial OTUs, with
105 diversity estimated to be around 1-2 orders of magnitude lower than their coral relatives, (Röthig
106 *et al.*, 2016; Herrera *et al.*, 2017). *Aiptasia* are easy to maintain, engage in a nutritive symbiosis
107 with Symbiodiniaceae similar to corals, and can reproduce asexually (Baumgarten *et al.*, 2015;
108 Weis, 2019). Unlike their coral relatives, *Aiptasia* can be rendered aposymbiotic (free of their
109 dinoflagellate algae) in laboratory conditions and lack a calcitic skeleton, which facilitates
110 experimental manipulation (Lehnert *et al.*, 2014).

111 While associations between microbial community composition and the abundance and/or
112 diversity of algal endosymbionts is consistent with the hypothesis that some microbes are
113 primary associates of Symbiodiniaceae, these patterns cannot be distinguished from passive
114 commensal relationships. Additionally, general stress may be responsible for changes in the host-
115 photosymbiont relationship, leading to alterations in metabolite production and resulting in
116 different selective pressures that favor distinct groups of commensals. For example,

117 Symbiodiniaceae taxa are known to differ in their metabolite production (Camp *et al.*, 2022).
118 *Durusdinium* translocates less carbon to hosts than *Cladocopium* (Cantin *et al.*, 2009) under
119 thermal stress but *Cladocopium* translocates more carbon and nitrogen to hosts during non-
120 stressful conditions (Pernice *et al.*, 2015), which could impact the consortium of microbiota in
121 the holobiont. The host-photosymbiont relationship can also be affected by mild bleaching,
122 which is another general stress response (Ortiz, Gomez-Cabrera and Hoegh-Guldberg, 2009).
123 Here, we aimed to distinguish the effects of the stress response and that of symbiont density on
124 microbial communities while controlling for host and symbiont genetic diversity. To achieve
125 this, we used the emerging model organism *Aiptasia* clonal strain CC7, which harbors
126 *Symbiodinium linucheae* (Starzak *et al.*, 2014; Baumgarten *et al.*, 2015) and conducted a
127 comparison between the microbiomes of symbiotic anemones undergoing mild bleaching and
128 aposymbiotic anemones, which were presumed to lack the microbes typically associated with
129 *Symbiodinium*.

130

131 MATERIALS AND METHODS

132 2.1 *Aiptasia* rearing

133 *Aiptasia* anemones, clone strain CC7 (obtained from Dr. Cory Krediet, Eckerd College, FL,
134 USA) were used in this study. Anemones were kept in 0.5 L polycarbonate tanks, filled with 0.2
135 μm filtered seawater (FSW) from Catalina Island (Catalina Water Co., Long Beach CA, USA)
136 and maintained at 25°C on a light/dark (14:10 h) cycle under 12-20 $\mu\text{mol photons m}^{-2} \text{ s}^{-1}$.
137 Animals were maintained in these common garden conditions at USC with weekly feeding
138 (frozen brine shrimp, *Artemia salina*) and water changes for 24 months. A subset of *Aiptasia*
139 animals were rendered aposymbiotic by menthol-induced bleaching (Matthews *et al.*, 2016) four
140 months prior to experimental trials. Briefly, a 1.28M menthol solution was prepared (20% w/v in
141 ethanol) and added to polycarbonate tanks containing FSW for a final concentration of 0.19
142 mmol l⁻¹. Anemones were placed in the menthol solution for 8 h during the light period of the
143 14:10, light: dark cycle. The animals were then transferred overnight to tanks containing a final
144 concentration of 0.10 M DCMU (3-(3,4-dichlorophenyl)-1,1-dimethylurea), an algicide and
145 photosynthesis inhibitor. This was repeated for four consecutive days. At the end of the fourth
146 day, anemones were placed in black-out tanks with no light exposure and allowed to recover for

147 three days with one feeding. After the three-day recovery, the process was repeated once more
148 and bleaching status was confirmed using a fluorescent microscope. An absence of red
149 autofluorescence from dinoflagellate chloroplasts was noted and these aposymbiotic anemones
150 were transferred to black-out tanks filled with 0.2 μm FSW and maintained in the dark for three
151 months with the same feeding and water change regime as the symbiotic anemone stock.

152 2.2 Experimental design and sampling

153 Symbiotic and aposymbiotic anemone of approximately 2.5 cm length were selected for the 6-
154 day thermal stress experiment. Aposymbiotic *Aiptasia* were added to the experimental design to
155 act as a control for distinguishing baseline host stress responses from cnidarian-algal microbiome
156 shifts. These aposymbiotic anemones were acclimated to the same light/dark (14:10 h) cycle as
157 symbiotic anemones one week prior to the experiment start date. In addition, all anemones were
158 starved for 2 weeks prior to sampling to avoid prey (shrimp, *Artemia sp.*) contamination.

159 Six 0.5 L tanks containing six symbiotic *Aiptasia* (n=36) and four 0.5 L tanks containing
160 six aposymbiotic *Aiptasia* (n=24) were distributed evenly between experimental conditions (25
161 $^{\circ}\text{C}$ vs 32 $^{\circ}\text{C}$, Fig. 1). The treatment temperature was set to 32 $^{\circ}\text{C}$ due to prior observation of
162 slight bleaching and expulsion of *Symbiodinium* in *Aiptasia* at this temperature (Perez, Cook and
163 Brooks, 2001)). To maintain and manipulate temperature, tanks used in the heat stress treatment
164 were placed in 10 L bins containing two SL381 submersible water pumps, two 100W aquarium
165 heaters, a HOBO temperature logger, and a digital, waterproof thermometer. Acclimatization of
166 *Aiptasia* was reached by exposing them to a gradual temperature ramp over the course of four
167 days. Temperature was increased from 25 ± 0.5 $^{\circ}\text{C}$ to 27 ± 0.5 $^{\circ}\text{C}$ the first day, to 30 ± 0.5 $^{\circ}\text{C}$
168 the second day, 32 ± 0.5 $^{\circ}\text{C}$ the third day and 33 ± 0.5 $^{\circ}\text{C}$ on the fourth day. Once *Aiptasia* were
169 acclimated to the elevated temperature treatment, treatment was maintained at an average of 32
170 ± 0.5 $^{\circ}\text{C}$ for 6 days with FSW changes every 2 days, in both control and heat-stress tanks. At the
171 end of the 6-day exposure period, each anemone was rinsed three times with FSW in individual
172 60 x 15 mm petri dishes, placed in a 1.5 mL microcentrifuge tube and frozen at -80 $^{\circ}\text{C}$, until
173 processing.

174

175 2.3 DNA extractions and 16S rDNA sequencing

176 Individual anemone DNA was extracted by ethanol precipitation as detailed previously
177 (https://openwetware.org/wiki/Ethanol_precipitation_of_nucleic_acids) with some
178 modifications. Briefly, animals were placed in sterile, 2 mL polypropylene screw cap tubes
179 (Merck KGaA, Germany) containing a thin layer of Zi/Si beads (100-500 μm diameter), 200 μL
180 lysis buffer AP1 from a DNEasy Power Plant Kit (Qiagen, Germany), 2 μL RNase (100 mg/mL,
181 stock), and 2 μL Proteinase K (20 mg/mL, stock) and incubated at 55 $^{\circ}\text{C}$ for 10 min in a
182 temperature-controlled water bath. Samples were then homogenized using the Omni bead beater
183 (Omni International, USA) at 6.3 m/s, for 2 cycles of 30 seconds. The samples were then
184 centrifuged for 5 min at 14,000 rpm and the proteinase K enzyme was heat-inactivated on a heat
185 block (78-82 $^{\circ}\text{C}$) for 3 min. The supernatant was transferred to a 1.5 mL microcentrifuge tube.
186 Ethanol precipitation was performed as described
187 (https://openwetware.org/wiki/Ethanol_precipitation_of_nucleic_acids) and the pellet was
188 resuspended in 40 μL elution buffer (GenElute Bacterial Genomic DNA Kit, Merck KGaA,
189 Germany). DNA was purified using the Zymo DNA Clean & Concentrator Kit (Zymo Research,
190 USA) following the manufacturer's instructions.

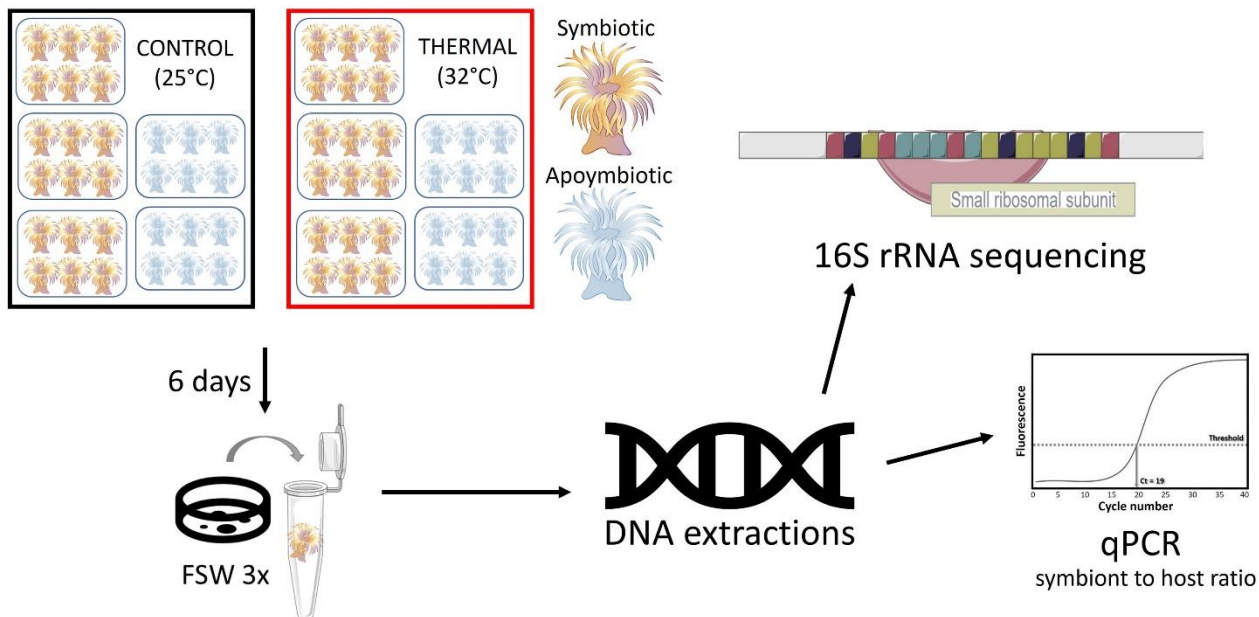


Figure 1. Study design for the mild thermal stress experiment. Each treatment condition received 5 tanks (3 tanks x 6 symbiotic anemones and 2 tanks x 6 aposymbiotic anemones; n= 30 per treatment). Following a 7-day ramping period, the peak temperature exposure continued for 6 days, and sampling was conducted on the last day. Each anemone was rinsed with filtered seawater (FSW) thrice, deposited into a microcentrifuge tube and stored at -80 $^{\circ}\text{C}$ until processing. DNA extractions were performed followed by 16S rRNA amplicon sequencing. Samples with remaining DNA were used in qPCR assays to determine symbiont (*Symbiodinium*) to host (*Aiptasia*) ratios.

191 Amplification of the V5/V6 region of the 16S rRNA gene was done using the 784F and
192 1061R primer set, which amplifies approximately 277 bp fragments with minor cross-
193 amplification of host mitochondria and microalgal symbiont chloroplasts (Andersson *et al.*,
194 2008; Bayer *et al.*, 2013). Briefly, 50 ng of DNA were amplified in 25 μ L reactions using 0.25 μ L
195 of 2,000 units/mL Q5 High-Fidelity DNA Polymerase (New England BioLabs Inc., Germany),
196 0.5 μ L of 10 mM each dNTP, 0.25 μ L of 10 μ M forward and reverse primer each, 0.25 μ L BSA
197 100X (New England BioLabs Inc., Germany), 5.0 μ L 5X Q5 PCR Buffer (New England
198 BioLabs Inc., Germany), 13.5 μ L nuclease-free water, and 5 μ L of 10 ng/ μ L DNA. PCR
199 conditions were as previously described in Bayer *et al.* (2013) with the following modifications:
200 26 cycles of denaturation at 95°C for 60 sec and annealing at 55°C for 60 sec. 5 μ L of the 16S
201 rRNA amplified sample was added to a second round of 3-step PCR to incorporate sample-
202 specific Illumina barcodes using an amplification profile of: 98°C 0:30, (98°C 0:10 | 59°C 0:30 |
203 72°C 0:30) x 4 cycles, 72°C 2:00. The barcoded samples were pooled in equimolar amounts (1
204 ng/ μ L) and sent for 250-bp paired-end sequencing on Illumina's MiSeq v2 PE 250 platform
205 (USC Norris Comprehensive Cancer Center Molecular Genomics Core (NCCC), USA).

206 2.4 16S rDNA sequencing and bioinformatic analysis

207 We successfully extracted DNA and sequenced the 16S rRNA gene of 59 individual anemones
208 (initial n=60) but seven samples were discarded from the dataset due to low read yields (<
209 2,000). Paired-end reads were demultiplexed by the sequencing facility (USC NCCC Molecular
210 Genomics Core) and quality checked with FastQC (Andrews, 2010). An amplicon sequencing
211 variant (ASV) table was generated with DADA2 (Callahan *et al.*, 2016) in R (R Core Team
212 2020) using the default filtering parameters (truncLen=c(240,160), maxN=0, maxEE=c(2,2),
213 truncQ=2, rm.phix=TRUE, compress=TRUE, multithread=FALSE). Taxonomy was assigned
214 using the Ribosomal Database Project Classifier (Wang *et al.*, 2007) along with the SILVA SSU
215 version 138.1 database, formatted for DADA2 (DOI/10.5281/zenodo.4587955). Chloroplast and
216 mitochondria sequences were removed using the R package, Phyloseq (McMurdie and Holmes,
217 2013). The dataset yielded uneven library sizes, so samples were rarefied to an even depth of 26,
218 481 reads (Gloor *et al.*, 2017; Weiss *et al.*, 2017). Following rarefaction, the dataset consisted of
219 1, 377, 012 reads (Table A1). All statistical analyses and visualizations were conducted in R (R
220 Core Team, 2020). Taxa plots, alpha diversity (Chao1 index), and beta-diversity visualizations

221 were conducted using the Phyloseq (McMurdie and Holmes, 2013), ggplot2 (Wilkinson, 2011),
222 and Microbiome (Lahti and Shetty *et al.*, 2019) packages. Differential tree matrices were
223 generated and visualized using the Metacoder (Foster, Sharpton and Grünwald, 2017) package.
224 Statistical output for differential heat trees can be found at Zenodo,
225 doi.org/10.5281/zenodo.7693398.

226 Additional statistical analyses were conducted using the vegan (Dixon, 2003) package. A
227 one-way ANOVA test was conducted on rarefied data, comparing alpha-diversity data (Chao1
228 scores) between the microbial assemblages of symbiotic and aposymbiotic anemone groups in
229 different treatments (control vs thermal stress). Post-hoc pairwise comparisons were done using
230 Tukey's HSD. Beta-diversity was visualized using a PCoA plot employing the weighted-Unifrac
231 metric. The adonis2 function in vegan was used to conduct pairwise Permutational Multivariate
232 Analysis of Variance (PERMANOVA) of microbial assemblage dissimilarities between
233 treatment groups. Adonis2 was used due to even homogeneity of variances in all pairwise
234 comparisons tested.

235 As the SILVA SSU v138.1 database only assigned some bacterial taxonomy to Order, we
236 conducted a separate phylogenetic analysis of ASVs classified in the order Oligoflexales. A
237 Bioconda (Grüning *et al.*, 2018) environment was used for this analysis. The filtered Phyloseq
238 dataset was subsetted to include only Oligoflexales reads and resulting ASVs were then
239 transferred to a fasta file and a standard NCBI nucleotide blast (Sayers *et al.*, 2023) was
240 performed on the web interface, optimizing for highly similar sequences (megablast). The ASVs
241 exhibited high quality (Table A2) matches to three uncultured bacterium clones, originating from
242 one microbial survey (Randle *et al.*, 2020) conducted on *Aiptasia* strain CC7 (GenBank:
243 MK571601.1/ MK571569.1) and *Aiptasia* strain H2 (GenBank: MK571216.1), as well as one
244 uncultured proteobacterium clone (GenBank: FJ425635) found in the microbiome of
245 scleractinian coral *Orbicella* (formerly *Montastrea*) *faveolata*. We queried our nine Oligoflexales
246 ASVs and these previously published sequences with 16S rDNA sequences from 2 confirmed
247 members of the Oligoflexales order (GenBank accession numbers AB540021.2 and
248 OW948931.1) and ten members (7 families) of the Bdellovibrionota phylum. Sequence
249 alignment was performed using the MUSCLE algorithm version 5.1 (Edgar, 2004) and a
250 phylogenetic tree was constructed by maximum likelihood with ultrafast bootstrap (n= 1,000

251 replicates) in IQ-TREE version 2.2.0.3 (Kalyaanamoorthy *et al.*, 2017; Minh *et al.*, 2020). The
252 resulting phylogenetic tree was visualized and annotated using the integrated web editor
253 interface, Interactive Tree of Life (ITOL, <https://itol.embl.de/>).

254 2.5 Symbiont to host (S/H) cell ratio qPCR

255 To assess the effects of thermal stress on symbiont density in *Aiptasia*, we analyzed symbiont to
256 host cell ratios (Mieog *et al.*, 2009) using nuclear ribosomal protein L10 as a reference gene for
257 the host, *Aiptasia* (Poole, Kitchen and Weis, 2016) and the actin locus as a target in
258 *Symbiodinium* (Palacio-Castro 2019). Nuclear ribosomal protein L10 primers were previously
259 validated for *Aiptasia* specificity in qPCR assays (Poole, Kitchen and Weis, 2016) and used as a
260 reference gene due to stable expression in *Aiptasia* (Kitchen and Weis, 2017). Previous qPCR
261 assays targeting the actin locus gene in *Symbiodinium* sp. (clade A) showed amplification
262 specificity with an estimated copy number for the actin locus at ~9 per cell (Palacio-Castro
263 2019). The primers used in this study for the host were 400nM nrp_L10-F (5'-
264 ACGTTTCTGCCGTGGTGTCCC-3') and 400 nM nrp_L10-R (5'-
265 CGGGCAGCTTCAAGGGCTTCA-3'). Primers used for *Symbiodinium* symbionts were 300 nM
266 Aact_F (5'-ATGAAGTGCGACGTGGACAT-3') and 200nM Aact_R (5'-
267 GGAGGACAGGATGGAGCCT-3'). All qPCR assays were performed on the Agilent AriaMx
268 qPCR Machine (Agilent, USA). Each reaction totaled 20 μ L volumes, using 10 μ L Brilliant III
269 Ultra-fast SYBR qPCR Master Mix (Agilent, USA), 6.1 μ L Milli-Q water, 0.8 μ L per primer
270 (forward and reverse, final concentrations listed above), 0.3 μ L 1:500 reference dye (SYBR) and
271 2 μ L of template DNA (concentration range between 5-10 ng/ μ L). The thermal profile was 50
272 $^{\circ}$ C 2:00, 95 $^{\circ}$ C 10:00 (95 $^{\circ}$ C 0:10 | 60 $^{\circ}$ C 1:00 | 72 $^{\circ}$ C 0.20) x 40 cycles + melt curve profile of
273 (95 $^{\circ}$ C 0:30 | 65 $^{\circ}$ C 0:30 | 95 $^{\circ}$ C 0:30) x 1 cycle. Due to low remaining DNA after 16S rRNA
274 library preparation and sequencing, we used 15 aposymbiotic replicates and 21 symbiotic
275 replicates (Table A3) for the qPCR assays. Each sample was assayed in duplicate, per target
276 primer set. Cycle threshold (Ct) values were calculated by Agilent AriaMx qPCR machine when
277 the first amplification cycle in a reaction exceeded the fluorescent baseline. All aposymbiotic
278 anemones in the control (but not those in the thermally stressed samples) exhibited non-target
279 amplification for the actin primer set, and upon analysis of the melt curve, we noticed a distinct
280 peak between 83-84 $^{\circ}$ C for these samples, yet all other positive amplification reactions exhibited

281 a distinct peak between 85-87 °C. We surmised cross-amplification of an *Aiptasia* locus in the
282 absence of a *Symbiodinium* target. Sanger sequencing of the different products revealed that actin
283 samples with a melt product between 85-86 °C exhibited high quality matches to the actin gene
284 locus in *Symbiodinium* spp. (GenBank: AB231899.1, NCBI nr BLAST, megablast, e-value= 8e-
285 86, bit score= 329) whereas no matches were identified for the lower melt product samples,
286 likely due to a high abundance of Ns in the sequences. Therefore, actin reactions exhibiting melt
287 products < 84 °C were assigned a cycle number of 40 to account for this non-specific
288 amplification (Table A4). Ct values were averaged between technical replicates and symbiont to
289 host ratios were calculated using the formula $((2^{-(Ct\ host)/(Ct\ sym)}) * 2)$ based on host/symbiont
290 target ploidy (*Aiptasia*, host = 2, *Symbiodinium*, symbiont = 1) (Cunning and Baker, 2013;
291 Palacio-Castro 2019).

292 2.6 S/H ratio statistical analyses

293 A dataset containing only symbiotic *Aiptasia* with S/H ratios, their alpha-diversity scores
294 (Shannon, Chao, Observed, Fisher and Simpson) and select bacterial abundance counts
295 (*Oligoflexales* and *Staphylococcus*) was used to generate a Pearson's correlation matrix using the
296 `corrplot` package in R (Wei and Simko, 2021). The `lm` command was used for regression analysis
297 of *Oligoflexales* abundance counts on S/H ratio in symbiotic anemones. We implemented a
298 linear mixed effects model with a fixed effect of treatment and a random effect of tank to test
299 whether S/H ratios were reduced in symbiotic anemones response to heat treatment using the
300 `nlme` (Pinheiro and Bates, 2023; Bates and Pinheiro, 1998), and `lme4` (Bates *et al.*, 2015)
301 packages.

302 RESULTS

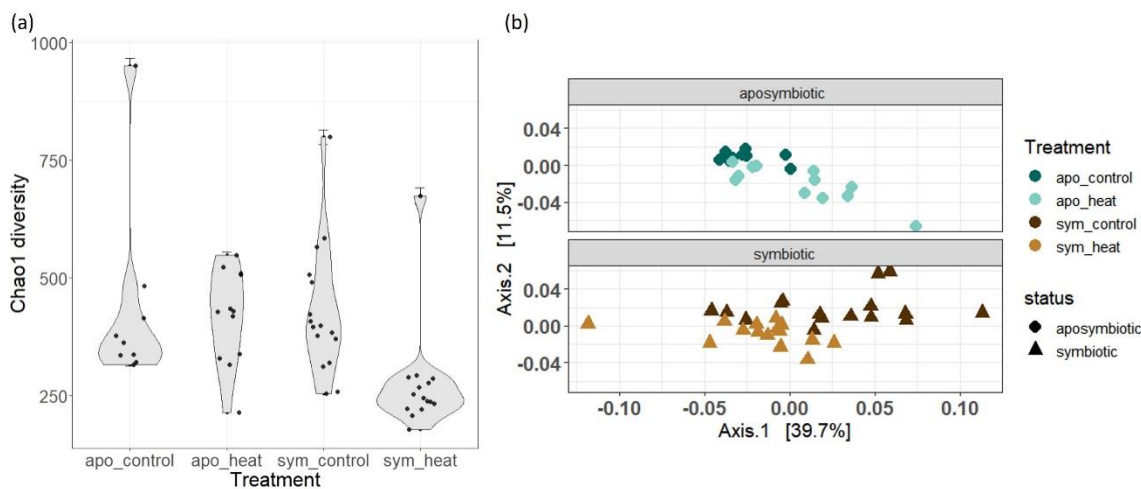
303 3.1 Microbial assemblages in *Aiptasia*

304 After ASV calling with DADA2, the sequence table yielded 4, 996, 356 reads and after
305 chloroplast and mitochondria removal, 4, 984, 116 reads and 4, 471 ASVs remained (Table A1).
306 Rarefaction and filtering of taxa occurring at least 3 times in more than 4 samples (the minimum
307 number of replicates per tank) yielded a final dataset of 1, 338, 082 reads and 774 ASVs. The
308 dataset was dominated by Alphaproteobacteria (66 %), Gammaproteobacteria (19%), and

309 Bdellovibrionota (4%) (Fig. A1). All other taxonomic classes were present in abundances < 3%,
310 except for Oligoflexia, which occurred at 4% relative abundance in symbiotic anemones under
311 control conditions (Fig. A1). The predominant genera in all samples were *Cognatishimia*, an
312 unnamed bacterium from the family Rhodobacteraceae and *Alcanivorax* (Fig. A2).

313 3.2 Community dynamics differ by treatment and symbiotic state

314 Alpha diversity was assessed by estimating species richness using the Chao1 index. Lower
315 within-sample diversity was observed in symbiotic anemones exposed to heat, but within-sample
316 diversity was consistent between other treatment groups (Fig. 2a). Although alpha diversity
317 differed between groups on average (ANOVA, $p=0.009$, Table A5), significant differences were
318 detected for only one pairwise comparison: heat-stressed symbiotic anemones and control
319 symbiotic anemones (Tukey multiple comparison of means, $p=0.016$, Table A5). A marginal
320 pairwise difference was detected between symbiotic and aposymbiotic anemones under heat
321 stress (Tukey multiple comparison of means, $p=0.05$, Table A5).



322 **Figure 2.** Alpha diversity and beta diversity differences of microbial assemblages in Aiptasia. (a) Alpha diversity index, Chao1, by treatment group. Standard error for Chao1 is represented by the error bars. (b) Beta differences by weighted Unifrac, principal coordinates of analysis (PCoA) on aposymbiotic samples (control, dark blue circles vs heat stressed, light blue circles) and symbiotic (control, dark brown triangles vs heat stressed, light brown triangles).

323 A principal coordinate analysis (PCoA, weighted Unifrac) also revealed differences in
324 beta diversity between symbiotic and aposymbiotic pairs in response to treatment (Fig. 2b).
325 Namely, beta diversity in heat-stressed symbiotic anemones converged whereas beta diversity in
326 control symbiotic anemones did not (PERMANOVA, $p= 0.001$, Table A6), indicating microbial
327 community composition in symbiotic anemones became more similar to each other after heat

328 treatment. The opposite pattern was observed in aposymbiotic anemones: convergence was
 329 observed in the control group and divergence in the heat treatment (Fig. 2b, PERMANOVA,
 330 $p=0.001$, Table A6). Differences in beta diversity were also observed between symbiotic and
 331 aposymbiotic animals under control conditions (ANOSIM $R=0.28$, $p=0.003$, Table A6).

332 We further explored taxa responsible for beta diversity disparities by generating a
 333 differential heat tree and visualizing statistically dissimilar taxa between pairwise comparisons.
 334 We detected differential abundance of several taxa (Wilcoxon Rank Sum tests, FDR-adjusted p -
 335 values <0.05 . Statistical output: Zenodo, doi.org/10.5281/zenodo.7693398) but most noticeably
 336 Firmicutes, Oligoflexales, Oceanospirillales, Planctomycetes and Alteromonadales (Fig. 3).
 337 Firmicute abundances were higher in aposymbiotic and symbiotic controls (Fig 3a, 3d), and
 338 Oligoflexales abundances were highest in symbiotic anemones under control conditions (Fig.
 339 3b). Bacteria from the family *Methylophilaceae* exhibited a similar pattern as Oligoflexales but
 340 overall abundance was low, and the difference between aposymbiotic and symbiotic controls was
 341 only ~ 100 raw counts. In contrast, Oligoflexales abundances in the aposymbiotic and symbiotic

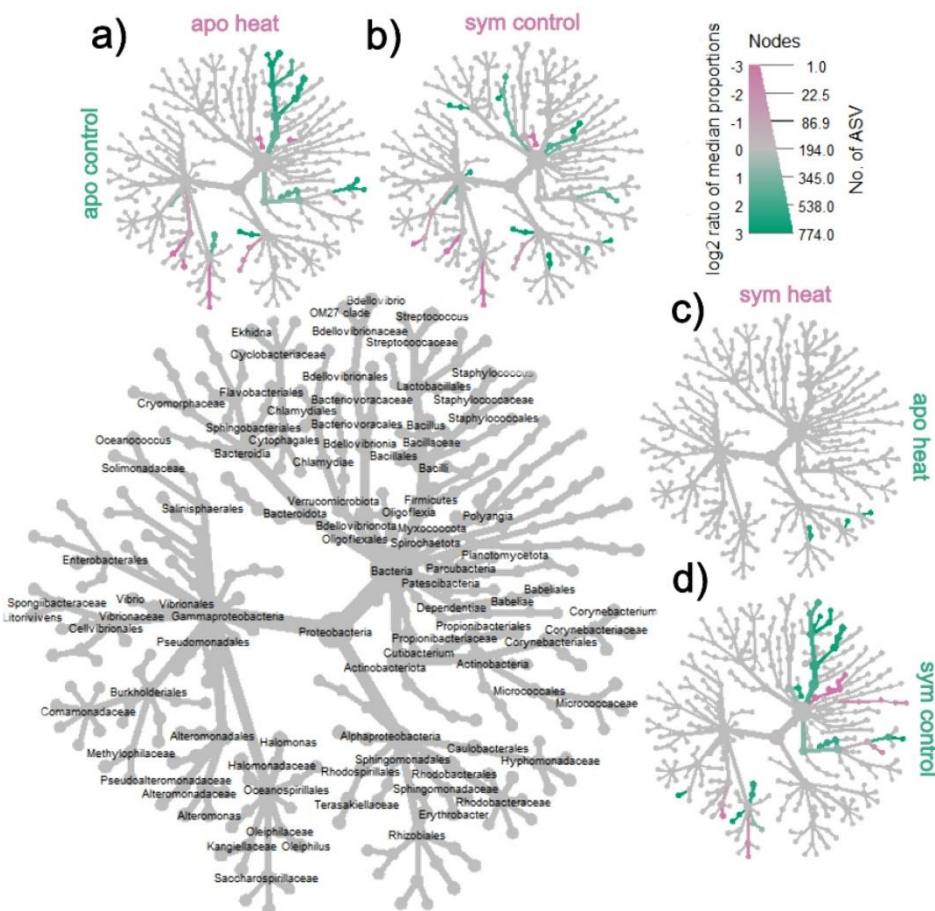


Figure 3. Differential heat trees illustrating pairwise comparisons between groups of interest. Amplicon data was used to visualize microbial taxonomic composition in *Aiptasia*, using the R package, Metacoder (Foster et al. 2017). The bigger tree with taxon labels on the lower left serves as a key for the smaller pairwise-comparison trees surrounding it a) aposymbiotic control vs aposymbiotic heat, b) aposymbiotic control vs symbiotic control, c) symbiotic heat-stressed vs aposymbiotic heat-stressed and d) symbiotic heat-stressed vs symbiotic control. Taxon color (diverging scheme from pink to green) is represented by log-2 ratio of median proportions of reads observed by treatment group. Significantly differentially abundant taxa, determined by Wilcoxon rank sum tests followed by FDR correction, colored in pink are more prominent in the groups shown in the columns and those colored in green are more prominent in the groups shown on the rows, e.g., Oligoflexales are significantly more abundant in symbiotic control (green) anemones than symbiotic heat-stressed but Myxococcota are enriched in symbiotic heat-stressed (pink). Size of tree nodes corresponds to ASV richness, as denoted in the color and size key in the upper right. Statistical output of differential abundance analysis is archived at Zenodo, doi.org/10.5281/zenodo.7693398

342 controls differed by 1-3 orders of magnitude (Fig. 4b). Alteromonadales and Oceanospirillales
343 abundance both decreased in heat-stressed anemones, regardless of symbiotic state (Fig. 3c).

344 3.3 Oligoflexales order are associated with symbiotic state and are lost under thermal stress

345 Oligoflexales abundances were elevated in symbiotic anemones under control conditions but
346 marginally elevated under heat treatment in aposymbiotic anemones relative to aposymbiotic
347 controls (Fig. 3a, 3b). Total abundance counts clearly displayed this categorical difference as
348 well (Fig. 4b). In addition to these categorical differences in Oligoflexales abundance by
349 anemone symbiotic state and treatment (Fig. A1, 3, 4b), we also observed quantitative
350 differences in abundance as a function of algal symbiont density. Symbiont to host (S/H) cell
351 ratios of symbiotic anemones decreased under thermal stress indicating mild bleaching ($p=0.047$,
352 Fig. A3, Table A7). Total S/H ratios for aposymbiotic anemones averaged around 0 but values
353 slightly increased in anemones exposed to thermal stress (Fig. A3, Table A4).

354 A correlation matrix was built to examine pairwise relationships between the S/H ratio of
355 symbiotic *Aiptasia*, alpha diversity, and Oligoflexales abundance counts. A moderate correlation
356 between S/H ratio and the abundance of Oligoflexales bacteria was detected (Pearson's
357 Correlation, $p=0.013$, Fig. A4, Table A8). Regression analysis verified this positive correlation,
358 revealing that 53% of the observed variation in Oligoflexales abundance across samples was
359 explained by differences in S/H ratio ($p < 0.001$, Fig. 4a).

360 3.4 Oligoflexales may diversify under thermal stress

361 A phylogenetic tree plotting Oligoflexales ASV abundance showed symbiotic anemones in
362 control conditions initially hosted 9 distinct ASVs but lost 1 after thermal stress (Fig. A5). In
363 contrast, aposymbiotic anemones only harbored 2 ASVs under control conditions, whereas 8
364 Oligoflexales ASVs were detected in aposymbiotic anemones which experienced thermal stress
365 (Fig. A5). We conducted a more detailed phylogenetic analysis to further investigate
366 relationships among these distinct ASVs and other Oligoflexales variants identified in prior
367 studies. Oligoflexales ASVs from this study grouped closely with three uncultured bacterium
368 clones originating from an unrelated study on *Aiptasia* clonal strains CC7 and H2 (Randle *et al.*,
369 2020) and one uncultured proteobacterium clone (GenBank: FJ425635) found in the microbiome

370 of the scleractinian coral *Orbicella* (formerly *Montastrea*) *faveolata* (Fig. A6). Other
371 Oligoflexales representatives were more distantly related (Fig. A6).

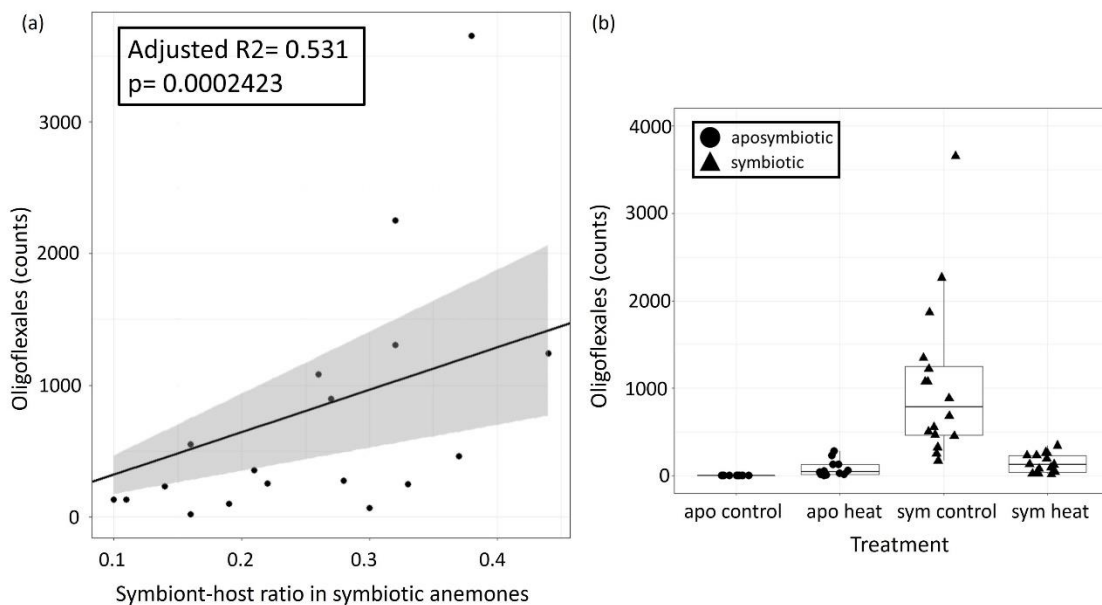


Figure 4. Oligoflexales in the microbiome of Aiptasia. (a) Regression line through the origin and linear model results testing the relationship between the dependent variable, Oligoflexales bacterial counts (y axis) and explanatory variable, symbiont to host ratio (S/H) (x axis). (b) Total counts of Oligoflexales in rarefied data, by treatment group (black circles= aposymbiotic anemones, black triangles= symbiotic anemones).

372

373 DISCUSSION

374 Overall, understanding the ecological dynamics of algal-microbe interactions in
375 cnidarians may be important for developing strategies to mitigate the impacts of climate change
376 (Matthews *et al.*, 2020). (Frommlet *et al.*, 2015) found that a diverse community of bacteria
377 facilitated the formation of symbiolites (spheroid, aragonite structures) in ex-hospite
378 Symbiodiniaceae cultures. This discovery highlighted a unique approach that could potentially
379 aid in coral calcification within reefs. Similarly, many eukaryotic algae are auxotrophs for the
380 prokaryote-produced B vitamins, like B12, and must obtain B12 from symbionts or dietary
381 sources for proper metabolic function and growth (Croft, Warren and Smith, 2006; Helliwell *et*
382 *al.*, 2011; Grossman, 2016). Furthermore, microbiome and algal symbiont co-occurrences may
383 be a result of metabolic cooperation, as dinoflagellates may rely on necessary metabolites
384 produced by bacteria and vice-versa (Cruz-López and Maske 2016; Grossman 2016; Kurihara *et*
385 *al.* 2013). Additional possible functional roles of bacteria associated with Symbiodiniaceae may
386 also span DMSP production, enhancing iron bioavailability and sulfur cycling (Lawson *et al.*

387 2018).

388

389 Here, we investigated the ecology of microbial communities, associated with *Aiptasia*,
390 and how they are affected by presence of the algal symbiont and elevated temperatures. Despite
391 treatment, Alphaproteobacteria and Gammaproteobacteria remained the predominant microbial
392 taxa. Differences in beta diversity were observed between symbiotic and aposymbiotic animals
393 under both control and thermal stress conditions but greater community similarity was observed
394 among microbial populations in both symbiotic and aposymbiotic anemones exposed to heat
395 stress. Additionally, elevated temperature decreased species richness in symbiotic anemones. We
396 also show that Oligoflexales bacteria are part of the rare microbiome in symbiotic anemones but
397 significantly decreased in abundance following thermal stress. The abundance of Oligoflexales
398 was positively correlated with higher S/H cell ratio indicating symbiont density, rather than heat
399 stress per se, impacted their abundance in *Aiptasia*.

400

401 **Exploring the cnidarian-algal-bacteria tripartite symbiosis, Oligoflexales as primary**
402 **associates of Symbiodiniaceae**

403

404 We examined the role of symbiotic algae in recruiting microbial taxa that may be specific to the
405 microbiomes of symbiotic *Aiptasia* and identified two taxa (Oligoflexales and *Methylophilaceae*)
406 that were significantly abundant in symbiotic *Aiptasia* only and decreased in relative abundance
407 with symbiont loss both independent of and as a result of thermal stress (Fig. 3b,3d; 4). We
408 focused on exploring Oligoflexales because these taxa were present in higher relative
409 abundances and had been previously reported as associates of *Aiptasia* (Randle *et al.*, 2020;
410 Maire, Blackall and van Oppen, 2021). Whereas we could not find a consistent record of
411 *Methylophilaceae* in symbiotic *Aiptasia*. Despite numerous surveys conducted on the *Aiptasia*
412 microbiome (Röthig *et al.*, 2016; Herrera *et al.*, 2017; Ahmed *et al.*, 2019; Hartman, van Oppen
413 and Blackall, 2020; Costa *et al.*, 2021), Oligoflexales remained undetected until recent research
414 reported their presence in *Aiptasia* strain CC7 (Randle *et al.*, 2020) and in the microbiome of
415 *Aiptasia* *acantia* in strains AIMS1, AIMS2, AIMS3, and AIMS4 (Maire, Blackall and van
416 Oppen, 2021). Two factors likely account for these results: (1) the utilization of identical
417 sequencing primer sets across all three studies, which document the existence of Oligoflexales,

418 including our own, and (2) the classification of taxonomy based on the most recent release of the
419 SILVA database (v138, issued in 2019). We chose to use the 784F/1061R primer set because it
420 captures global bacterial diversity while exhibiting low amplification of chloroplast and
421 mitochondrial host DNA (Bayer *et al.*, 2013; Andersson *et al.*, 2008; Bayer *et al.*, 2013) (Bayer
422 *et al.*, 2013). Furthermore, as Oligoflexales were recently recognized as a novel order under the
423 Bdellovibrionota phylum (Nakai *et al.*, 2014; Waite *et al.*, 2020)), older databases may designate
424 them as “unclassified/uncultured bacterial clones”. Based on our research and the prior studies,
425 we conclude that Oligoflexales are a consistent component of the symbiotic microbiome in
426 Aiptasia.

427

428 Bacteria belonging to the Oligoflexales order are Gram-negative, oligotrophic
429 spirochaetes, and only one species, *Oligoflexus tunisiensis*, has been described and isolated
430 (Nakai *et al.*, 2014, 2016). We conducted a phylogenetic analysis of nine Oligoflexales ASV
431 sequences against *O. tunisiensis* and other members of the parent phylum, Bdellovibrionota
432 (Waite *et al.*, 2020). Our ASVs formed a sister clade to *O. tunisiensis* and *Pseudobacteriovorax*
433 *antilogorgiicola*, an isolate from gorgonian corals in the family Pseudobacteriovoracacea
434 (McCauley, Haltli and Kerr, 2015) (Fig. A6). This suggests a close relationship between them.
435 Currently, Pseudobacteriovoracacea are classified as Bdellovibrionales, but a proposal to
436 reclassify them as Oligoflexales was submitted (Hahn *et al.*, 2017), which is consistent with our
437 findings grouping them with *O. tunisiensis*.

438

439 Although the ecological role of Oligoflexales in symbiotic Aiptasia remains a mystery, it
440 has previously been suggested to comprise a set of taxa that aid thermotolerance in high salinities
441 (Randle *et al.*, 2020). The genome sequence of *O. tunisiensis* also provides clues on possible
442 metabolic capabilities in Oligoflexales. Nakai *et al.* (2016) observed an incomplete
443 denitrification pathway in *O. tunisiensis*, which resulted in the conversion of nitrate/nitrite
444 (NO_3/NO_2) to nitrous oxide (N_2O). Heterotrophic bacteria are known to recycle fixed nitrogen
445 from the environment through denitrification, and those with a complete pathway can reduce
446 fixed nitrogen to dinitrogen (N_2) gas (Knowles, 1982). Nitrogen recycling by the host, Aiptasia,
447 regulates algal symbiotic density (Cui *et al.*, 2019) but bacterially regulated nitrogen may play a
448 role in maintenance of the cnidarian-algal symbiosis as well, since nitrogen cycling is a hallmark

449 of reciprocal bacterial association in cnidarian holobionts (Knowlton and Rohwer, 2003; Peixoto
450 *et al.*, 2017). It is unclear if the Oligoflexiales in the present study possess a similar
451 denitrification pathway, but the genomic evidence from *O. tunisiensis* suggests that further
452 research is needed to investigate this possibility.

453
454 We observed a higher abundance of Oligoflexiales ASVs in symbiotic Aiptasia under
455 control conditions, compared to symbiotic animals in the heat-stress treatment. In contrast,
456 aposymbiotic Aiptasia in the control showed only 1 ASV but experienced an increase in diversity
457 and abundance of ASVs in thermally stressed, aposymbiotic anemones (Fig. A5). While
458 superficially this observation initially appears to contradict the notion that Oligoflexiales are
459 associates of Symbiodiniaceae, we believe this pattern can be explained by the dynamics of
460 symbiont maintenance and proliferation in Aiptasia (Jinkerson *et al.*, 2022) and is actually fully
461 consistent with the primary algal symbiont hypothesis.

462
463 Aposymbiotic Aiptasia anemones can retain remnant populations of algal symbionts,
464 even in the absence of light. *S. linuchae* do not need to photosynthesize to be maintained in
465 Aiptasia in dark conditions (Jinkerson *et al.*, 2022). Jinkerson et al (2022) also found that *S.*
466 *linuchae* did not proliferate *in-hospite* in the dark, but algal cell density significantly increased
467 after subsequent transition to light conditions. We theorize that a small, non-detectable (by PCR)
468 population of algal symbionts remained in the aposymbiotic group, despite continuous darkness
469 for three months. This *S. linuchae* population likely proliferated during the combined light and
470 heat-stress periods as confirmed by the slight increase in S/H ratios in this population (Fig. A3,
471 Table A4), in contrast to the aposymbiotic controls only exposed to light. A recent study showed
472 significantly higher proliferation of *S. linuchae* in Aiptasia at 32 °C, after 28 days compared to
473 ambient temperatures (25 °C), suggesting cell division rates initially increased in response to
474 elevated temperature but then declined after 12 weeks of sustained thermal stress (Herrera *et al.*,
475 2021). The slight increase in algal abundance in the aposymbiotic population subjected to
476 thermal stress was concomitant with an increase and diversification of Oligoflexiales (Fig 4b, Fig
477 A5). Whereas the opposite pattern (Oligoflexiales loss) was observed in symbiotic Aiptasia
478 exposed to heat stress. S/H ratios were lower (Table A4, Fig. A3) in symbiotic anemones
479 exposed to thermal stress, and significant differences were observed between treatments (Table

480 A7), indicating symbiont loss. Thermal stress can promote bleaching in symbiotic cnidarians
481 leading to dysbiosis (Weis, 2008; Wooldridge, 2009)) but the mechanisms are not thoroughly
482 established. One theory suggests dysbiosis may occur as a cascade effect that begins with a
483 decrease in the photosynthetic efficiency of the symbiont, followed by a reduction in ammonium
484 assimilation by the host, leading to an increase in the available ammonium pool. This, in turn,
485 stimulates algal growth, and eventually, the host becomes unable to keep up with the resulting
486 internal metabolic shifts, leading to the expulsion of the symbionts (Cui *et al.*, 2019; Rådecker *et*
487 *al.*, 2021). We hypothesize that heat-stressed, aposymbiotic *Aiptasia* did not experience the same
488 metabolic constraints and were able to adequately support growth of algal populations, leading to
489 slightly higher symbiont abundance and increased abundance/diversity of Oligoflexales bacteria
490 (Fig. 4b, Fig. A5).

491
492 Lastly, it is a possibility that Oligoflexales observed in aposymbiotic anemones under
493 heat conditions were environmentally acquired. We used 0.2 μm FSW to maintain our cultures
494 but previous research has demonstrated that *O. tunisiensis* is part of the 0.2 μm filtrate culturable
495 fraction (Nakai *et al.*, 2014). Although *O. tunisiensis* can reach up to 10 μm in length, and are
496 between 0.4 - 0.8 μm wide, they can compress through 0.2 μm filter pores. We do not have
497 morphological data for the Oligoflexales in this study, so we cannot eliminate the possibility of
498 environmental contamination. However, all animals were clonal propagates and were maintained
499 using 0.2 μm FSW, originating from the same 20 L tank, yet displayed distinct microbiome
500 profiles according to treatment (Fig 3). Furthermore, the disparity of Oligoflexales abundances
501 between treatment groups (Fig. 4b) indicates symbiotic-state specificity in control conditions.
502 Environmentally acquired or not, Oligoflexales may play an important role in the holobiont as
503 endosymbiotic partners that only associate with cnidarians when microalgal symbionts are
504 present, as rare members of the symbiotic microbiome. It is possible that Oligoflexales, like rare
505 members of the coral core microbiome, are widespread in anemone tissue, particularly in close
506 proximity to algal symbionts (D Ainsworth *et al.*, 2015) and future work should aim to fully
507 characterize their abundance and distribution.

508
509
510

511 **Microbiome assemblages of aposymbiotic and symbiotic Aiptasia**

512

513 Microbial assemblages in Aiptasia from wild and cultured populations (including clonal strain
514 CC7) in ambient conditions showed consistent similarity at the phylum level but not at lower
515 taxonomic levels (Brown *et al.*, 2017). In all our samples, regardless of treatment, *Alcanivorax*
516 sp. from the Oceanospirillales order, *Cognatishimia* sp., and an unclassified bacterium from the
517 Rhodobacteraceae family from the Rhodobacterales order accounted for around 60-85% of the
518 total relative abundance (Fig. A2). This observation, that 2-3 taxa are numerically dominant in
519 Aiptasia, contradicts other microbial surveys on Aiptasia that identified a wider range of
520 taxonomic groups within the same relative abundance range (Röthig *et al.*, 2016; Randle *et al.*,
521 2020; Curtis *et al.*, 2023). The importance of functional redundancy in shaping microbial
522 communities in Aiptasia is emphasized by the conflicting results obtained from various studies.
523 Functional redundancy refers to a diverse range of bacteria with similar capabilities, able to
524 perform similar functions in the same niche (Louca *et al.*, 2018). Functional redundancy is an
525 advantageous strategy for ecosystem stability and may play a role in the resilience of hosts, like
526 corals, facing environmental disturbances (Voolstra and Ziegler, 2020).

527

528 Prior work conducted by (Röthig *et al.*, 2016; Ahmed *et al.*, 2019; Randle *et al.*, 2020)
529 showed that aposymbiotic and symbiotic Aiptasia (CC7), hosted distinct microbiomes. Here we
530 expanded upon this finding by introducing a stressor to assess the response of the aposymbiotic
531 microbiome and the symbiotic microbiome under thermal stress (Fig. A1). Although alpha-
532 diversity did not differ between symbiotic status (Fig. 2a), beta-diversity was dissimilar (Fig. 2b,
533 Table A6), which prompted us to explore which taxa were responsible for these observations.
534 We observed a significant difference in the relative abundance of Oligoflexales,
535 Saccharospirillaceae, Pseudoalteromonadaceae, and Methylophilaceae families between
536 symbiotic and aposymbiotic animals, with these taxa being more prevalent in the former (Fig.
537 3b). Our findings align with other studies that have demonstrated differences in relative
538 abundance of microbiome composition between aposymbiotic and symbiotic states in strain CC7
539 (Röthig *et al.*, 2016; Sydnor, 2020; Curtis *et al.*, 2023). Nevertheless, the four differentially
540 abundant taxa we identified were not previously reported, suggesting genotype by environment
541 and symbiotic state all influence microbial assemblages in Aiptasia.

542 **Microbiome fluctuations caused by heat stress changed the rare microbiome**

543

544 Here, we aimed to identify microbial taxa that are linked with symbiotic states in a defined
545 clonal strain of *Aiptasia* and tracked microbial fluctuations of these taxa following mild
546 bleaching. The dominant taxa in all *Aiptasia* were found to be unaffected by both temperature
547 and symbiotic state. However, the rare microbiome of symbiotic *Aiptasia* was significantly
548 affected by temperature stress. In contrast to the other treatment groups, symbiotic *Aiptasia*
549 exhibited a reduction in alpha-diversity and beta-diversity convergence after six days of exposure
550 to heat stress (Fig. 2). A decrease in alpha-diversity was also observed in another study exposing
551 symbiotic *Aiptasia* CC7 to short-term heat stress (Sydnor, 2020), but it appears to be a temporary
552 phenomenon since a long-term study by (Ahmed *et al.*, 2019) on *Aiptasia* CC7, surveying
553 microbial communities under continuous heat stress (32°C for two years) demonstrated an
554 increase in both alpha-diversity and number of bacterial taxa relative to paired controls. Here,
555 symbiotic *Aiptasia* experienced microbiome restructuring when subjected to heat stress (Fig. 3d)
556 and the resulting assemblage was most similar to that observed in heat-stressed aposymbiotic
557 anemones (Fig. 3c). This suggests that short-term heat stress in *Aiptasia* may be the main driver
558 that led to a convergence of microbial communities in both aposymbiotic and symbiotic animals.

559

560 However, possible symbiont gains in the aposymbiotic and symbiont loss in the
561 symbiotic anemones exposed to thermal stress (Fig. A3) may also be contributing to the
562 convergence of microbial communities. Symbiotic anemones exhibited increased relative
563 abundance of several bacteria taxa, most noticeably *Oligoflexales*, *Saccharospirillaceae*, and
564 *Pseudoalteromonadaceae* compared to aposymbiotic anemones under control temperatures (Fig.
565 3b). These same taxa increase in relative abundance in heat-stressed aposymbiotic anemones
566 compared to control aposymbiotic anemones (Fig. 3a) until their relative abundance is
567 indistinguishable from those observed in the symbiotic anemones in response to thermal stress
568 (Fig. 3c). Whereas their abundances decrease in response to heat stress in symbiotic anemones
569 (Fig. 3d). The most parsimonious explanation for these apparently contradictory changes in
570 response to heat stress is that it is not thermal stress, but algal symbiont density which influences
571 patterns of convergence. Additional time-course studies examining repopulation of algal
572 symbiont communities would provide additional support for this hypothesis.

573 It is unclear whether changes in the relative abundance or composition of the microbial
574 community affected the physiology or fitness of aposymbiotic and symbiotic *Aiptasia* hosts as
575 we did not conduct any host-specific assays, but we can confirm that no *Aiptasia* died during the
576 course of this experiment. While we have identified a strong association between the abundance
577 of *Oligoflexales* and algal endosymbionts independent of thermal stress, whether these bacteria
578 are mutualists or commensals remains unresolved. Additional work on patterns of localization,
579 metabolic exchange, and spatial and temporal fidelity are needed. But given the tractability of the
580 *Aiptasia* model, this represents a promising future study system for investigating multi-partner
581 symbioses. Understanding how the absence of a member in a multipartite symbiosis impacts the
582 resilience of other organisms in the holobiont can uncover valuable insights into how symbiotic
583 organisms respond to environmental challenges.

584 **ACKNOWLEDGEMENTS**

585 This study was funded by the National Science Foundation Graduate Research Fellowship
586 Program grant award DGE-1418060 to EGA and start-up funding from the University of
587 Southern California to CDK. We would like to thank Dr. Cory J Krediet for providing a set of
588 clonal *Aiptasia* CC7 anemones. Special thanks to Dr. Ross Cunning, Dr. Sheila Kitchen and Dr.
589 Angela Poole for invaluable assistance in determining appropriate qPCR primers. Additionally,
590 we would like to thank Daniel Olivares-Zambrano for help pooling the libraries before
591 sequencing and Maria Ruggeri for kindly providing *Aiptasia* CC7 DNA samples to test the qPCR
592 primers used to calculate symbiont to host ratios.

593 **CONFLICT OF INTEREST**

594 The authors declare no competing interests.

595 **AUTHOR CONTRIBUTIONS**

596 EGA and CDK conceived and designed the field experiment and obtained funding. EGA and
597 MJF performed anemone maintenance, aposymbiotic generation and sampling for the
598 experiment. EGA completed DNA extractions, library preparation, qPCR and all bioinformatic
599 and statistical analyses and wrote the first draft of the manuscript. All authors contributed to

600 revisions.

601 **DATA ACCESSIBILITY**

602 Scripts for data analysis and statistical output for differential heat trees generated using the
603 Metacoder R package are archived at Zenodo, doi.org/10.5281/zenodo.7693398. It can also be
604 viewed at https://github.com/symbiotic-em/aiptasia_thermal_stress. Demultiplexed sequences
605 are available at the National Center for Biotechnology Information (NCBI) Sequence Read
606 Archives (SRA) under accession code: [PRJNA929535](https://www.ncbi.nlm.nih.gov/sra/PRJNA929535).

607 **ORCID ID**

608 Emily G. Aguirre ([0000-0002-4846-4109](https://orcid.org/0000-0002-4846-4109))

609 Carly D. Kenkel ([0000-0003-1126-4311](https://orcid.org/0000-0003-1126-4311))

610 **REFERENCES**

611 Adeniji, A.A., Babalola, O.O. and Loots, D.T. (2020) ‘Metabolomic applications for understanding complex
612 tripartite plant-microbes’ interactions: Strategies and perspectives’, *Biotechnology reports (Amsterdam,
613 Netherlands)*, 25, p. e00425. Available at: <https://doi.org/10.1016/j.btre.2020.e00425>.

614 Afkhami, M.E. *et al.* (2020) ‘Tripartite mutualisms as models for understanding plant-microbial interactions’,
615 *Current opinion in plant biology*, 56, pp. 28–36. Available at: <https://doi.org/10.1016/j.pbi.2020.02.003>.

616 Ahmed, H.I. *et al.* (2019) ‘Long-Term Temperature Stress in the Coral Model *Aiptasia* Supports the “Anna
617 Karenina Principle” for Bacterial Microbiomes’, *Frontiers in Microbiology*. Available at:
618 <https://doi.org/10.3389/fmicb.2019.00975>.

619 Allemand, D. and Osborn, D. (2019) ‘Ocean acidification impacts on coral reefs: From sciences to solutions’,
620 *Regional Studies in Marine Science*, p. 100558. Available at: <https://doi.org/10.1016/j.rsma.2019.100558>.

621 Andersson, A.F. *et al.* (2008) ‘Comparative analysis of human gut microbiota by barcoded pyrosequencing’, *PLoS
622 one*, 3(7), p. e2836. Available at: <https://doi.org/10.1371/journal.pone.0002836>.

623 Andrews, S. (2010). FastQC: A Quality Control Tool for High Throughput Sequence Data [Online]. Available at:
624 <http://www.bioinformatics.babraham.ac.uk/projects/fastqc/>.

625 Anon, 2020. Anaconda Software Distribution, Anaconda Inc. Available at: <https://docs.anaconda.com/>.

626 Antunes, P.M. and Goss, M.J. (2015) ‘Communication in the Tripartite Symbiosis Formed by Arbuscular
627 Mycorrhizal Fungi, Rhizobia and Legume Plants: A Review’, *Roots and Soil Management: Interactions between
628 Roots and the Soil*, pp. 199–222. Available at: <https://doi.org/10.2134/agronmonogr48.c11>.

629 Barno, A.R. *et al.* (2021) ‘Host under epigenetic control: A novel perspective on the interaction between
630 microorganisms and corals’, *BioEssays: news and reviews in molecular, cellular and developmental biology*, 43(10),
631 p. e2100068. Available at: <https://doi.org/10.1002/bies.202100068>.

632 Bates, D. *et al.* (2015) ‘Fitting Linear Mixed-Effects Models Using **lme4**’, *Journal of Statistical Software*. Available

- 633 at: <https://doi.org/10.18637/jss.v067.i01>.
- 634 Bates, D.M. and Pinheiro, J.C. (1998) 'LINEAR AND NONLINEAR MIXED-EFFECTS MODELS', *Conference*
635 *on Applied Statistics in Agriculture* [Preprint]. Available at: <https://doi.org/10.4148/2475-7772.1273>.
- 636 Baumgarten, S. *et al.* (2015) 'The genome of *Aiptasia*, a sea anemone model for coral symbiosis', *Proceedings of*
637 *the National Academy of Sciences of the United States of America*, 112(38), pp. 11893–11898. Available at:
638 <https://doi.org/10.1073/pnas.1513318112>.
- 639 Bayer, T. *et al.* (2013) 'The microbiome of the Red Sea coral *Stylophora pistillata* is dominated by tissue-associated
- 640 *Endozoicomonas* bacteria', *Applied and environmental microbiology*, 79(15), pp. 4759–4762. Available at:
641 <https://doi.org/10.1128/AEM.00695-13>.
- 642 Bernasconi, R. *et al.* (2019) 'Global Networks of Symbiodinium-Bacteria Within the Coral Holobiont', *Microbial*
643 *ecology*, 77(3), pp. 794–807. Available at: <https://doi.org/10.1007/s00248-018-1255-4>.
- 644 Blackall, L.L., Wilson, B. and van Oppen, M.J.H. (2015) 'Coral—the world's most diverse symbiotic ecosystem',
645 *Molecular ecology*, 24(21), pp. 5330–5347. Available at: <https://doi.org/10.1111/mec.13400>.
- 646 Boucher, D.H. (1985) *The Biology of Mutualism: Ecology and Evolution*. Oxford University Press on Demand.
647 Available at: https://books.google.com/books/about/The_Biology_of_Mutualism.html?hl=&id=dWuQS_3F2P0C.
- 648 Bourne, D.G., Morrow, K.M. and Webster, N.S. (2016) 'Insights into the Coral Microbiome: Underpinning the
- 649 Health and Resilience of Reef Ecosystems', *Annual review of microbiology*, 70, pp. 317–340. Available at:
650 <https://doi.org/10.1146/annurev-micro-102215-095440>.
- 651 Brown, T. *et al.* (2017) 'Worldwide exploration of the microbiome harbored by the cnidarian model, *Exaiptasia*
- 652 *pallida* (Agassiz in Verrill, 1864) indicates a lack of bacterial association specificity at a lower taxonomic rank',
653 *PeerJ*, 5, p. e3235. Available at: <https://doi.org/10.7717/peerj.3235>.
- 654 Callahan, B.J. *et al.* (2016) 'DADA2: High-resolution sample inference from Illumina amplicon data', *Nature*
655 *methods*, 13(7), pp. 581–583. Available at: <https://doi.org/10.1038/nmeth.3869>.
- 656 Camp, E.F. *et al.* (2022) 'Proteome metabolome and transcriptome data for three Symbiodiniaceae under ambient
- 657 and heat stress conditions', *Scientific data*, 9(1), p. 153. Available at: <https://doi.org/10.1038/s41597-022-01258-w>.
- 658 Cantin, N.E. *et al.* (2009) 'Juvenile corals can acquire more carbon from high-performance algal symbionts', *Coral*
659 *reefs*, 28(2), pp. 405–414. Available at: <https://doi.org/10.1007/s00338-009-0478-8>.
- 660 Chaston, J. and Goodrich-Blair, H. (2010) 'Common trends in mutualism revealed by model associations between
- 661 invertebrates and bacteria', *FEMS microbiology reviews*, 34(1), pp. 41–58. Available at:
662 <https://doi.org/10.1111/j.1574-6976.2009.00193.x>.
- 663 Cleveland, A., Alan Verde, E. and Lee, R.W. (2011) 'Nutritional exchange in a tropical tripartite symbiosis: direct
- 664 evidence for the transfer of nutrients from anemonefish to host anemone and zooxanthellae', *Marine Biology*, pp.
665 589–602. Available at: <https://doi.org/10.1007/s00227-010-1583-5>.
- 666 Costa, R.M. *et al.* (2021) 'Surface Topography, Bacterial Carrying Capacity, and the Prospect of Microbiome
- 667 Manipulation in the Sea Anemone Coral Model *Aiptasia*', *Frontiers in microbiology*, 12, p. 637834. Available at:
668 <https://doi.org/10.3389/fmicb.2021.637834>.
- 669 Croft, M.T., Warren, M.J. and Smith, A.G. (2006) 'Algae need their vitamins', *Eukaryotic cell*, 5(8), pp. 1175–1183.
670 Available at: <https://doi.org/10.1128/EC.00097-06>.
- 671 Cui, G. *et al.* (2019) 'Host-dependent nitrogen recycling as a mechanism of symbiont control in *Aiptasia*', *PLoS*
672 *genetics*, 15(6), p. e1008189. Available at: <https://doi.org/10.1371/journal.pgen.1008189>.

- 673 Cuning, R. and Baker, A.C. (2013) ‘Excess algal symbionts increase the susceptibility of reef corals to bleaching’,
674 *Nature Climate Change*, pp. 259–262. Available at: <https://doi.org/10.1038/nclimate1711>.
- 675 Curtis, E. *et al.* (2023) ‘Bacterial microbiome variation across symbiotic states and clonal lines in a cnidarian
676 model’, *Frontiers in Marine Science*. Available at: <https://doi.org/10.3389/fmars.2023.1113043>.
- 677 D Ainsworth, T. *et al.* (2015) ‘The coral core microbiome identifies rare bacterial taxa as ubiquitous
678 endosymbionts’, *The ISME journal*, 9(10), pp. 2261–2274. Available at: <https://doi.org/10.1038/ismej.2015.39>.
- 679 Dixon, G.B. *et al.* (2015) ‘CORAL REEFS. Genomic determinants of coral heat tolerance across latitudes’, *Science*,
680 348(6242), pp. 1460–1462. Available at: <https://doi.org/10.1126/science.1261224>.
- 681 Dixon, P. (2003) ‘VEGAN, a package of R functions for community ecology’, *Journal of Vegetation Science*, pp.
682 927–930. Available at: <https://doi.org/10.1111/j.1654-1103.2003.tb02228.x>.
- 683 Douglas, A.E. (2003) ‘Coral bleaching--how and why?’, *Marine pollution bulletin*, 46(4), pp. 385–392. Available at:
684 [https://doi.org/10.1016/S0025-326X\(03\)00037-7](https://doi.org/10.1016/S0025-326X(03)00037-7).
- 685 Drury, C. (2020) ‘Resilience in reef-building corals: The ecological and evolutionary importance of the host
686 response to thermal stress’, *Molecular ecology*, 29(3), pp. 448–465. Available at:
687 <https://doi.org/10.1111/mec.15337>.
- 688 Edgar, R.C. (2004) ‘MUSCLE: a multiple sequence alignment method with reduced time and space complexity’,
689 *BMC bioinformatics*, 5, p. 113. Available at: <https://doi.org/10.1186/1471-2105-5-113>.
- 690 Ffrench-Constant, R.H., Eleftherianos, I. and Reynolds, S.E. (2007) ‘A nematode symbiont sheds light on
691 invertebrate immunity’, *Trends in parasitology*, 23(11), pp. 514–517. Available at:
692 <https://doi.org/10.1016/j.pt.2007.08.021>.
- 693 Foster, Z.S.L., Sharpton, T.J. and Grünwald, N.J. (2017) ‘Metacoder: An R package for visualization and
694 manipulation of community taxonomic diversity data’, *PLOS Computational Biology*, p. e1005404. Available at:
695 <https://doi.org/10.1371/journal.pcbi.1005404>.
- 696 Frommlet, J.C. *et al.* (2015) ‘Coral symbiotic algae calcify ex hospite in partnership with bacteria’, *Proceedings of
697 the National Academy of Sciences of the United States of America*, 112(19), pp. 6158–6163. Available at:
698 <https://doi.org/10.1073/pnas.1420991112>.
- 699 Gloor, G.B. *et al.* (2017) ‘Microbiome Datasets Are Compositional: And This Is Not Optional’, *Frontiers in
700 microbiology*, 8, p. 2224. Available at: <https://doi.org/10.3389/fmicb.2017.02224>.
- 701 Grossman, A. (2016) ‘Nutrient Acquisition: The Generation of Bioactive Vitamin B 12 by Microalgae’, *Current
702 Biology*, pp. R319–R321. Available at: <https://doi.org/10.1016/j.cub.2016.02.047>.
- 703 Grüning, B. *et al.* (2018) ‘Bioconda: sustainable and comprehensive software distribution for the life sciences’,
704 *Nature methods*, 15(7), pp. 475–476. Available at: <https://doi.org/10.1038/s41592-018-0046-7>.
- 705 Gupta, S. *et al.* (2021) ‘Alleviation of salinity stress in plants by endophytic plant-fungal symbiosis: Current
706 knowledge, perspectives and future directions’, *Plant and Soil*, pp. 219–244. Available at:
707 <https://doi.org/10.1007/s11104-020-04618-w>.
- 708 Hahn, M.W. *et al.* (2017) ‘*Silvanigrella aquatica* gen. nov., sp. nov., isolated from a freshwater lake, description of
709 *Silvanigrellaceae* fam. nov. and *Silvanigrellales* ord. nov., reclassification of the order *Bdellovibrionales* in the class
710 *Oligoflexia*, reclassification of the families *Bacteriovoracaceae* and *Halobacteriovoracaceae* in the new order
711 *Bacteriovoracales* ord. nov., and reclassification of the family *Pseudobacteriovoracaceae* in the order *Oligoflexales*’,
712 *International journal of systematic and evolutionary microbiology*, 67(8), pp. 2555–2568. Available at:
713 <https://doi.org/10.1099/ijsem.0.001965>.

- 714 Hartman, L.M., van Oppen, M.J.H. and Blackall, L.L. (2020) ‘Microbiota characterization of *Exaiptasia diaphana*
715 from the Great Barrier Reef’, *Animal microbiome*, 2(1), p. 10. Available at: [https://doi.org/10.1186/s42523-020-](https://doi.org/10.1186/s42523-020-00029-5)
716 00029-5.
- 717 Helliwell, K.E. *et al.* (2011) ‘Insights into the evolution of vitamin B12 auxotrophy from sequenced algal genomes’,
718 *Molecular biology and evolution*, 28(10), pp. 2921–2933. Available at: <https://doi.org/10.1093/molbev/msr124>.
- 719 Herrera, M. *et al.* (2017) ‘Laboratory-Cultured Strains of the Sea Anemone *Exaiptasia* Reveal Distinct Bacterial
720 Communities’, *Frontiers in Marine Science*. Available at: <https://doi.org/10.3389/fmars.2017.00115>.
- 721 Herrera, M. *et al.* (2021) ‘Temperature transcends partner specificity in the symbiosis establishment of a cnidarian’,
722 *The ISME journal*, 15(1), pp. 141–153. Available at: <https://doi.org/10.1038/s41396-020-00768-y>.
- 723 Hoegh-Guldberg, O. *et al.* (2007) ‘Coral reefs under rapid climate change and ocean acidification’, *Science*,
724 318(5857), pp. 1737–1742. Available at: <https://doi.org/10.1126/science.1152509>.
- 725 Jinkerson, R.E. *et al.* (2022) ‘Cnidarian-Symbiodiniaceae symbiosis establishment is independent of
726 photosynthesis’, *Current biology: CB*, 32(11), pp. 2402–2415.e4. Available at:
727 <https://doi.org/10.1016/j.cub.2022.04.021>.
- 728 Kalyaanamoorthy, S. *et al.* (2017) ‘ModelFinder: fast model selection for accurate phylogenetic estimates’, *Nature*
729 *methods*, 14(6), pp. 587–589. Available at: <https://doi.org/10.1038/nmeth.4285>.
- 730 Kitchen, S.A. and Weis, V.M. (2017) ‘The sphingosine rheostat is involved in the cnidarian heat stress response but
731 not necessarily in bleaching’, *Journal of Experimental Biology* [Preprint]. Available at:
732 <https://doi.org/10.1242/jeb.153858>.
- 733 Kleypas, J.A.A. and Kleypas, J.A.K. (2019) ‘Climate change and tropical marine ecosystems: A review with an
734 emphasis on coral reefs’, *UNED Research Journal*, pp. S24–S35. Available at:
735 <https://doi.org/10.22458/urj.v1i1.2317>.
- 736 Knowles, R. (1982) ‘Denitrification’, *Microbiological Reviews*, pp. 43–70. Available at:
737 <https://doi.org/10.1128/mr.46.1.43-70.1982>.
- 738 Knowlton, N. and Rohwer, F. (2003) ‘Multispecies microbial mutualisms on coral reefs: the host as a habitat’, *The*
739 *American naturalist*, 162(4 Suppl), pp. S51–62. Available at: <https://doi.org/10.1086/378684>.
- 740 Lahti, L., Shetty S., *et al.* (2017). ‘Tools for microbiome analysis in R.’ Available at:
741 <https://microbiome.github.com/microbiome>
- 742 Lam, V.W.Y. *et al.* (2020) ‘Climate change, tropical fisheries and prospects for sustainable development’, *Nature*
743 *Reviews Earth & Environment*, pp. 440–454. Available at: <https://doi.org/10.1038/s43017-020-0071-9>.
- 744 Lehnert, E.M. *et al.* (2014) ‘Extensive differences in gene expression between symbiotic and aposymbiotic
745 cnidarians’, *G3*, 4(2), pp. 277–295. Available at: <https://doi.org/10.1534/g3.113.009084>.
- 746 Louca, S. *et al.* (2018) ‘Function and functional redundancy in microbial systems’, *Nature ecology & evolution*,
747 2(6), pp. 936–943. Available at: <https://doi.org/10.1038/s41559-018-0519-1>.
- 748 Maire, J., Blackall, L.L. and van Oppen, M.J.H. (2021) ‘Microbiome characterization of defensive tissues in the
749 model anemone *Exaiptasia diaphana*’, *BMC microbiology*, 21(1), p. 152. Available at:
750 <https://doi.org/10.1186/s12866-021-02211-4>.
- 751 Mather, J. (2013) ‘Marine Invertebrates: Communities at Risk’, *Biology*, pp. 832–840. Available at:
752 <https://doi.org/10.3390/biology2020832>.
- 753 Matthews, J.L. *et al.* (2016) ‘Menthol-induced bleaching rapidly and effectively provides experimental

- 754 aposymbiotic sea anemones (*Aiptasia* sp.) for symbiosis investigations’, *The Journal of experimental biology*,
755 219(Pt 3), pp. 306–310. Available at: <https://doi.org/10.1242/jeb.128934>.
- 756 Matthews, J.L. *et al.* (2020) ‘Symbiodiniaceae-bacteria interactions: rethinking metabolite exchange in reef-building
757 corals as multi-partner metabolic networks’, *Environmental microbiology*, 22(5), pp. 1675–1687. Available at:
758 <https://doi.org/10.1111/1462-2920.14918>.
- 759 McCauley, E.P., Haltli, B. and Kerr, R.G. (2015) ‘Description of *Pseudobacteriovorax antillogorgiicola* gen. nov.,
760 sp. nov., a bacterium isolated from the gorgonian octocoral *Antillogorgia elisabethae*, belonging to the family
761 *Pseudobacteriovoracaceae* fam. nov., within the order *Bdellovibrionales*’, *International Journal of Systematic and*
762 *Evolutionary Microbiology*, pp. 522–530. Available at: <https://doi.org/10.1099/ijs.0.066266-0>.
- 763 McMurdie, P.J. and Holmes, S. (2013) ‘phyloseq: An R Package for Reproducible Interactive Analysis and
764 Graphics of Microbiome Census Data’, *PLoS ONE*, p. e61217. Available at:
765 <https://doi.org/10.1371/journal.pone.0061217>.
- 766 Mieog, J.C. *et al.* (2009) ‘Quantification of algal endosymbionts (Symbiodinium) in coral tissue using real-time
767 PCR’, *Molecular ecology resources*, 9(1), pp. 74–82. Available at: [https://doi.org/10.1111/j.1755-](https://doi.org/10.1111/j.1755-0998.2008.02222.x)
768 [0998.2008.02222.x](https://doi.org/10.1111/j.1755-0998.2008.02222.x).
- 769 Minh, B.Q. *et al.* (2020) ‘IQ-TREE 2: New Models and Efficient Methods for Phylogenetic Inference in the
770 Genomic Era’, *Molecular Biology and Evolution*, pp. 1530–1534. Available at:
771 <https://doi.org/10.1093/molbev/msaa015>.
- 772 Miransari, M. (2011) ‘Arbuscular mycorrhizal fungi and nitrogen uptake’, *Archives of Microbiology*, pp. 77–81.
773 Available at: <https://doi.org/10.1007/s00203-010-0657-6>.
- 774 Nakai, R. *et al.* (2014) ‘*Oligoflexus tunisiensis* gen. nov., sp. nov., a Gram-negative, aerobic, filamentous bacterium
775 of a novel proteobacterial lineage, and description of *Oligoflexaceae* fam. nov., *Oligoflexales* ord. nov. and
776 *Oligoflexia* classis nov’, *International Journal of Systematic and Evolutionary Microbiology*, pp. 3353–3359.
777 Available at: <https://doi.org/10.1099/ijs.0.060798-0>.
- 778 Nakai, R. *et al.* (2016) ‘Genome sequence and overview of *Oligoflexus tunisiensis* Shr3T in the eighth class
779 *Oligoflexia* of the phylum *Proteobacteria*’, *Standards in Genomic Sciences*. Available at:
780 <https://doi.org/10.1186/s40793-016-0210-6>.
- 781 Olson, N.D. *et al.* (2009) ‘Diazotrophic bacteria associated with Hawaiian *Montipora* corals: Diversity and
782 abundance in correlation with symbiotic dinoflagellates’, *Journal of Experimental Marine Biology and Ecology*, pp.
783 140–146. Available at: <https://doi.org/10.1016/j.jembe.2009.01.012>.
- 784 van Oppen, M.J.H. and Blackall, L.L. (2019) ‘Coral microbiome dynamics, functions and design in a changing
785 world’, *Nature Reviews Microbiology*, pp. 557–567. Available at: <https://doi.org/10.1038/s41579-019-0223-4>.
- 786 Ortiz, J.C., Gomez-Cabrera, M. del C. and Hoegh-Guldberg, O. (2009) ‘Effect of colony size and surrounding
787 substrate on corals experiencing a mild bleaching event on Heron Island reef flat (southern Great Barrier Reef,
788 Australia)’, *Coral reefs*, 28(4), pp. 999–1003. Available at: <https://doi.org/10.1007/s00338-009-0546-0>.
- 789 Palacio-Castro, A. M. (2019). ‘Abiotic controls on endosymbiotic algal communities and their implications for coral
790 bleaching susceptibility and recovery’, (Doctoral dissertation, University of Miami).
- 791 Pandolfi, J.M. *et al.* (2003) ‘Global trajectories of the long-term decline of coral reef ecosystems’, *Science*,
792 301(5635), pp. 955–958. Available at: <https://doi.org/10.1126/science.1085706>.
- 793 Peixoto, R.S. *et al.* (2017) ‘Beneficial Microorganisms for Corals (BMC): Proposed Mechanisms for Coral Health
794 and Resilience’, *Frontiers in microbiology*, 8, p. 341. Available at: <https://doi.org/10.3389/fmicb.2017.00341>.
- 795 Perez, S.F., Cook, C.B. and Brooks, W.R. (2001) ‘The role of symbiotic dinoflagellates in the temperature-induced

- 796 bleaching response of the subtropical sea anemone *Aiptasia pallida*, *Journal of experimental marine biology and*
797 *ecology*, 256(1), pp. 1–14. Available at: [https://doi.org/10.1016/s0022-0981\(00\)00282-3](https://doi.org/10.1016/s0022-0981(00)00282-3).
- 798 Pernice, M. *et al.* (2015) ‘A nanoscale secondary ion mass spectrometry study of dinoflagellate functional diversity
799 in reef-building corals’, *Environmental microbiology*, 17(10), pp. 3570–3580. Available at:
800 <https://doi.org/10.1111/1462-2920.12518>.
- 801 Pinheiro J., Bates D. (2023). ‘nlme: Linear and Nonlinear Mixed Effects Models. R package version 3.1-162, R
802 Core Team’. Available at <https://CRAN.R-project.org/package=nlme>.
- 803 Poole, A.Z., Kitchen, S.A. and Weis, V.M. (2016) ‘The Role of Complement in Cnidarian-Dinoflagellate Symbiosis
804 and Immune Challenge in the Sea Anemone *Aiptasia pallida*’, *Frontiers in microbiology*, 7, p. 519. Available at:
805 <https://doi.org/10.3389/fmicb.2016.00519>.
- 806 Räddecker, N. *et al.* (2021) ‘Heat stress destabilizes symbiotic nutrient cycling in corals’, *Proceedings of the National*
807 *Academy of Sciences of the United States of America*, 118(5). Available at:
808 <https://doi.org/10.1073/pnas.2022653118>.
- 809 Randle, J.L. *et al.* (2020) ‘Salinity-Conveyed Thermotolerance in the Coral Model *Aiptasia* Is Accompanied by
810 Distinct Changes of the Bacterial Microbiome’, *Frontiers in Marine Science*. Available at:
811 <https://doi.org/10.3389/fmars.2020.573635>.
- 812 Reshef, L. *et al.* (2006) ‘The coral probiotic hypothesis’, *Environmental microbiology*, 8(12), pp. 2068–2073.
813 Available at: <https://doi.org/10.1111/j.1462-2920.2006.01148.x>.
- 814 Ritchie, K.B. (2012) ‘Bacterial Symbionts of Corals and Symbiodinium’, *Beneficial Microorganisms in*
815 *Multicellular Life Forms*, pp. 139–150. Available at: https://doi.org/10.1007/978-3-642-21680-0_9.
- 816 Röthig, T. *et al.* (2016) ‘Distinct Bacterial Communities Associated with the Coral Model *Aiptasia* in Aposymbiotic
817 and Symbiotic States with Symbiodinium’, *Frontiers in Marine Science*. Available at:
818 <https://doi.org/10.3389/fmars.2016.00234>.
- 819 Rouzé, H. *et al.* (2016) ‘Symbiodinium clades A and D differentially predispose *Acropora cytherea* to disease and
820 *Vibrio* spp. colonization’, *Ecology and Evolution*, pp. 560–572. Available at: <https://doi.org/10.1002/ece3.1895>.
- 821 Sachs, J.L. *et al.* (2004) ‘The evolution of cooperation’, *The Quarterly review of biology*, 79(2), pp. 135–160.
822 Available at: <https://doi.org/10.1086/383541>.
- 823 Santoyo, G. *et al.* (2022) *Mitigation of Plant Abiotic Stress by Microorganisms: Applicability and Future*
824 *Directions*. Academic Press. Available at: <https://play.google.com/store/books/details?id=V6BMEAAAQBAJ>.
- 825 Sayers, E.W. *et al.* (2023) ‘Database resources of the National Center for Biotechnology Information in 2023’,
826 *Nucleic acids research*, 51(D1), pp. D29–D38. Available at: <https://doi.org/10.1093/nar/gkac1032>.
- 827 Smith, J.M. and Szathmary, E. (1997) *The Major Transitions in Evolution*. Oxford University Press. Available at:
828 https://books.google.com/books/about/The_Major_Transitions_in_Evolution.html?hl=&id=Qts6FAcGGaIC.
- 829 Starzak, D.E. *et al.* (2014) ‘The influence of symbiont type on photosynthetic carbon flux in a model cnidarian–
830 dinoflagellate symbiosis’, *Marine Biology*, pp. 711–724. Available at: <https://doi.org/10.1007/s00227-013-2372-8>.
- 831 Stock, S.P. (2019) ‘Partners in crime: symbiont-assisted resource acquisition in *Steinernema* entomopathogenic
832 nematodes’, *Current opinion in insect science*, 32, pp. 22–27. Available at:
833 <https://doi.org/10.1016/j.cois.2018.10.006>.
- 834 Sydnor, J.R. (2020) *The Bacterial Community Associated with the Model Sea Anemone *Exaiptasia Pallida*:*
835 *Response to Rising Ocean Temperature*. Available at:
836 https://books.google.com/books/about/The_Bacterial_Community_Associated_with.html?hl=&id=WICfzwEACAJ.

- 837 Thomas, L. *et al.* (2018) ‘Mechanisms of Thermal Tolerance in Reef-Building Corals across a Fine-Grained
838 Environmental Mosaic: Lessons from Ofu, American Samoa’, *Frontiers in Marine Science*. Available at:
839 <https://doi.org/10.3389/fmars.2017.00434>.
- 840 University of Massachusetts Amherst Massachusetts Lynn Margulis, Margulis, L. and Fester, R. (1991) *Symbiosis
841 as a Source of Evolutionary Innovation: Speciation and Morphogenesis*. MIT Press. Available at:
842 https://books.google.com/books/about/Symbiosis_as_a_Source_of_Evolutionary_In.html?hl=&id=3sKzeiHUIUQC.
- 843 Voolstra, C.R. and Ziegler, M. (2020) ‘Adapting with Microbial Help: Microbiome Flexibility Facilitates Rapid
844 Responses to Environmental Change’, *BioEssays: news and reviews in molecular, cellular and developmental
845 biology*, 42(7), p. e2000004. Available at: <https://doi.org/10.1002/bies.202000004>.
- 846 Wahida, A., Tang, F. and Barr, J.J. (2021) ‘Rethinking phage-bacteria-eukaryotic relationships and their influence
847 on human health’, *Cell host & microbe*, 29(5), pp. 681–688. Available at:
848 <https://doi.org/10.1016/j.chom.2021.02.007>.
- 849 Waite, D.W. *et al.* (2020) ‘Proposal to reclassify the proteobacterial classes and the phylum into four phyla
850 reflecting major functional capabilities’, *International journal of systematic and evolutionary microbiology*, 70(11),
851 pp. 5972–6016. Available at: <https://doi.org/10.1099/ijsem.0.004213>.
- 852 Wang, Q. *et al.* (2007) ‘Naive Bayesian classifier for rapid assignment of rRNA sequences into the new bacterial
853 taxonomy’, *Applied and environmental microbiology*, 73(16), pp. 5261–5267. Available at:
854 <https://doi.org/10.1128/AEM.00062-07>.
- 855 Wei, T. and Simko, V. (2021) R Package “Corrplot”: Visualization of a Correlation Matrix. Available at:
856 <https://github.com/taiyun/corrplot>
857
- 858 Weiss, S. *et al.* (2017) ‘Normalization and microbial differential abundance strategies depend upon data
859 characteristics’, *Microbiome*, 5(1), p. 27. Available at: <https://doi.org/10.1186/s40168-017-0237-y>.
- 860 Weis, V.M. (2008) ‘Cellular mechanisms of Cnidarian bleaching: stress causes the collapse of symbiosis’, *The
861 Journal of experimental biology*, 211(Pt 19), pp. 3059–3066. Available at: <https://doi.org/10.1242/jeb.009597>.
- 862 Weis, V.M. (2019) ‘Cell Biology of Coral Symbiosis: Foundational Study Can Inform Solutions to the Coral Reef
863 Crisis’, *Integrative and Comparative Biology*, pp. 845–855. Available at: <https://doi.org/10.1093/icb/icz067>.
- 864 Wichard, T. (2015) ‘Exploring bacteria-induced growth and morphogenesis in the green macroalga order Ulvales
865 (Chlorophyta)’, *Frontiers in plant science*, 6, p. 86. Available at: <https://doi.org/10.3389/fpls.2015.00086>.
- 866 Wilkinson, L. (2011) ‘ggplot2: Elegant Graphics for Data Analysis by WICKHAM, H’, *Biometrics*, pp. 678–679.
867 Available at: <https://doi.org/10.1111/j.1541-0420.2011.01616.x>.
- 868 Wooldridge, S.A. (2009) ‘A new conceptual model for the warm-water breakdown of the coral - algae
869 endosymbiosis’, *Marine and Freshwater Research*, p. 483. Available at: <https://doi.org/10.1071/mf08251>.
- 870 Worthen, P.L., Gode, C.J. and Graf, J. (2006) ‘Culture-independent characterization of the digestive-tract microbiota
871 of the medicinal leech reveals a tripartite symbiosis’, *Applied and environmental microbiology*, 72(7), pp. 4775–
872 4781. Available at: <https://doi.org/10.1128/AEM.00356-06>.
- 873 Zan, J. *et al.* (2019) ‘A microbial factory for defensive kahalalides in a tripartite marine symbiosis’, *Science*.
874 Available at: <https://doi.org/10.1126/science.aaw6732>.